Scattering and Bound States of Quasiparticles at the A-B Phase Boundary of Superfluid ^{3}He

N. Schopohl and D. Waxman[a]
Institut Laue-Langevin, 156X, 38042 Grenoble CEDEX, France
(Received 3 October 1988)

The boundary between the A and B phases of superfluid ^{3}He possesses many interesting features due to the drastically different bulk order parameters. We study the transmission and Andreev reflection of ballistic wave packets of excitations incident on the A-B phase boundary. We find that the A-B phase boundary is magnetically active and capable of converting an unpolarized incident wave packet into partially polarized transmitted and Andreev-reflected wave packets. We also consider equilibrium properties due to bound states and resonances of excitations localized near the phase boundary. These states contribute to magnetic correlations and to mass and spin currents flowing in the plane of the interface.

PACS numbers: 67.50.Fi

Superfluid ^{3}He is known to exist in two quite distinct phases: the A and the B phase. In each phase the total spin S and the orbital angular momentum L of the Cooper pairs are unity. However, in the A phase the pairs are oriented along a common angular momentum direction $\hat{\mathbf{l}}$. The result is that the A phase is highly anisotropic, in contrast to the B phase which is isotropic in the absence of orienting fields.[1]

It is well known that the quasiparticle excitations in the bulk superfluid phases of ^{3}He are coherent superpositions of particles and holes. Depending on the dominance of the particle (hole) character of a wave packet of such excitations, it will propagate parallel (antiparallel) to the Fermi velocity v_F. A richer behavior is found when the order parameter undergoes a rapid variation on a length scale comparable to the coherence length. Such a variation occurs, for example, at the A-B phase boundary where the two phases coexist.[2,3]

In the present work we consider a planar A-B phase boundary lying in the $x=0$ plane. We model the exact profile of the order parameter[4] by a piecewise-constant complex vector

$$\Delta(x,\hat{\mathbf{k}}) = \begin{cases} \Delta_A \hat{\mathbf{k}}\cdot(\hat{\boldsymbol{\phi}}_{\mathrm{I}} + i\hat{\boldsymbol{\phi}}_{\mathrm{II}})\hat{\mathbf{w}} & \text{for } x<0 \\ \Delta_B \hat{\mathbf{k}} & \text{for } x>0, \end{cases} \tag{1}$$

where $\hat{\boldsymbol{\phi}}_{\mathrm{I}} + i\hat{\boldsymbol{\phi}}_{\mathrm{II}} = \hat{\mathbf{x}} + i\hat{\mathbf{z}}$, $\hat{\mathbf{w}} = \hat{\mathbf{x}}$, $\hat{\mathbf{l}} = \hat{\boldsymbol{\phi}}_{\mathrm{I}} \times \hat{\boldsymbol{\phi}}_{\mathrm{II}} = -\hat{\mathbf{y}}$ as illustrated in Fig. 1. This correctly describes the known asymptotic orientation of the order parameter in equilibrium and provides an adequate description for phenomena occurring on length scales large compared with the thickness $\Lambda \simeq 3\xi$ of the phase boundary. We note that the $\hat{\mathbf{d}}$ vector of the A phase is related to $\hat{\mathbf{w}}$ via $\hat{\mathbf{w}} = \overleftrightarrow{R}(\theta,\hat{\mathbf{n}})\cdot\hat{\mathbf{d}}$, where the parameters θ and $\hat{\mathbf{n}}$ of the rotation matrix $\overleftrightarrow{R}$ follow from minimization of the dipole energy.[4,5]

In what follows we determine waves of low-energy excitations moving in the order parameter, Eq. (1). We work to quasiclassical accuracy, in the limit of a low excitation density, and neglect quasiparticle collisions.[6,7] With these restrictions the advanced, retarded, and Keldysh propagators $\{g^A, g^R, g^K\}$ of the quasiclassical theory all obey the same transportlike differential equation[6,8]:

$$iv_F\hat{\mathbf{k}}\cdot\nabla g(\mathbf{R},t;\hat{\mathbf{k}},\epsilon) + [\mathcal{H},g]_- + (i/2)[\tau_3,\partial_t g]_+ = 0. \tag{2}$$

Apart from satisfying the above equation $g^{R(A)}$ is subject to the necessary condition of analyticity in the upper (lower) complex ϵ plane. In equilibrium ($\partial_t g = 0$) the propagators are related by $g^K_{\mathrm{eq}} = \tanh(\epsilon/2T)[g^R_{\mathrm{eq}} - g^A_{\mathrm{eq}}]$, where T is the absolute temperature. Furthermore,[8] $g^R_{\mathrm{eq}} g^R_{\mathrm{eq}} = -\pi^2 = g^A_{\mathrm{eq}} g^A_{\mathrm{eq}}$.

The elementary excitations described by g are characterized by four labels specifying particles and holes with spin up and down. A complete specification furthermore requires ϵ, the deviation from the Fermi energy, and $\hat{\mathbf{k}}$, a unit vector giving the direction of the excitation momentum at position $\mathbf{R}$ and time t (further details are given in Ref. 8).

It follows that g, $\mathcal{H}$, and τ_3 are 4×4 matrices, the last two given in 2×2 sub-block form as

$$\mathcal{H} = \begin{pmatrix} \epsilon & \Delta \\ -\Delta^\dagger & -\epsilon \end{pmatrix}, \quad \tau_3 = \begin{pmatrix} 1 & 0 \\ 0 & -1 \end{pmatrix}$$

with

$$\Delta = \sum_{\mu=1}^{3} \Delta_\mu(x,k)\sigma^\mu i\sigma^2.$$

We note that Eq. (2) is deceptively simple. In component form it represents 16 coupled complex partial

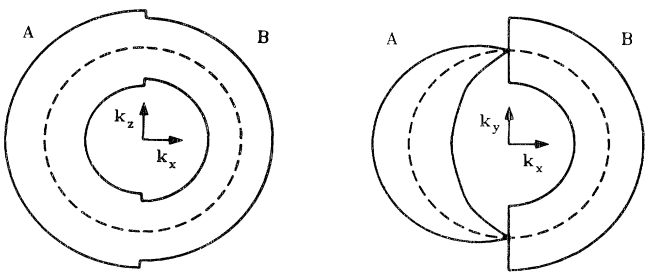

FIG. 1. Schematic cross sections of the Fermi sphere (dashed lines) indicating the maximum and minimum bulk gaps on either side of the A-B interface.

differential equations. However, because we work with a piecewise-constant order parameter the general solution of Eq. (2) may be derived in closed form; on either side of the interface it is given by the compact formula

$$g(\mathbf{R},t;\hat{\mathbf{k}},\epsilon)=\int_{-\infty}^{\infty}\frac{d\omega}{d\pi}K(\omega)\begin{bmatrix}\tilde{C}_{11}e^{i\{[\mathbf{k}(\omega)-\mathbf{k}(-\omega)]\cdot\mathbf{R}-\omega t\}} & \tilde{C}_{12}e^{i\{[\mathbf{k}(\omega)+\mathbf{k}(-\omega)]\cdot\mathbf{R}-\omega t\}}\\ \tilde{C}_{21}e^{-i\{[\mathbf{k}(\omega)+\mathbf{k}(-\omega)]\cdot\mathbf{R}+\omega t\}} & \tilde{C}_{22}e^{-i\{[\mathbf{k}(\omega)-\mathbf{k}(-\omega)]\cdot\mathbf{R}+\omega t\}}\end{bmatrix}K(-\omega)\,. \tag{3}$$

This result, which lies at the core of this paper, requires some explanation; details of its derivation may be found in Ref. 9. Firstly, the wave vectors $\mathbf{k}(\omega)$ are given by $\mathbf{k}(\omega)=\hat{\mathbf{k}}E(\omega)/v_F$, where $\pm E(\omega)$ are eigenvalues of $\mathcal{H}+(\omega/2)\tau_3$ and $E(\omega)=[(\epsilon+\omega/2)^2-\Delta\cdot\Delta^*]^{1/2}$. The phases $\mathbf{k}(\omega)-\mathbf{k}(-\omega)]\cdot\mathbf{R}\pm\omega t$ describe waves of excitations propagating along $\mp\hat{\mathbf{k}}$, while the phases $[\mathbf{k}(\omega)+\mathbf{k}(-\omega)]\cdot\mathbf{R}\pm\omega t$ describe nonpropagating waves due to their different symmetry under $\omega\rightarrow-\omega$.

Secondly, the transformation $K(\omega)$ has the properties

$$K(\omega)[\mathcal{H}+(\omega/2)\tau_3]k(\omega)=E(\omega)\tau_3,\quad K(\omega)K(\omega)=1\,.$$

It is given by

$$K(\omega)=\frac{[E(\omega+\omega/2]\tau_3+\mathcal{H}}{\{2E(\omega)[E(\omega)+\omega/2+\epsilon]\}^{1/2}}\,.$$

Thirdly, the 2×2 blocks $\tilde{C}_{mn}$ depend on which side of the interface they are evaluated [like all the other quantities appearing in Eq. (3)]. It is important to note that they are functions of $\hat{\mathbf{k}}\times\mathbf{R}$ and ω.

If we consider propagating waves incident from the B phase onto the interface ($\hat{\mathbf{k}}\cdot\hat{\mathbf{x}}<0$), then in the A phase these can only lead to waves propagating away from the interface, provided $|\epsilon|>\max(\Delta_B,\Delta_A|\hat{\mathbf{k}}\times\hat{\boldsymbol{l}}|)$. This implies that in the A phase,

$$\tilde{C}^A_{12}=\tilde{C}^A_{21}=\tilde{C}^A_{22}=0\,.$$

Furthermore, correct matching of the two pieces of the propagator at the interface, $x=0$, requires

$$\tilde{C}^A_{11}=C^A_{11}e^{-i(\hat{\mathbf{k}}\times\mathbf{b}^A_{11})\cdot\mathbf{R}},$$
$$\tilde{C}^B_{mn}=C^B_{mn}e^{-i(\hat{\mathbf{k}}\times\mathbf{b}^B_{mn})\cdot\mathbf{R}},$$

where the weights C^A_{11} and C^B_{mn} are independent of $\mathbf{R}$. Given that $\mathbf{b}^B_{11}\equiv\mathbf{0}$ for waves incident from the B phase, the remaining $\mathbf{b}$ vectors follow from continuity in y and z at the interface at $x=0$.

The weight C^B_{11} determines the character of the incoming quasiparticles, namely the shape of their wave packet, their number, and their spin. Similarly C^A_{11} characterizes the transmitted quasiparticles. The Andreev reflection excitations[10] with group velocity approximately antiparallel to $\hat{\mathbf{k}}$ are described by C^B_{22}. The off-diagonal weights C^B_{12} and C^B_{21} correspond to the interference between the incoming and Andreev-reflected quasiparticle and do not represent propagating modes. All initial information of the scattering problem is contained in C^B_{11}. Indeed, the remaining 2×2 blocks C^B_{mn},C^A_{11} can, from continuity, be expressed in terms of C^B_{11} with the use of the matrix products $K^B(\omega)K^A(\omega)$ and $K^A(-\omega)\times K^B(-\omega)$ representing the overlap of the transformation matrices $K(\omega)$. Expanded details are given in Ref. 9.

Having outlined our procedure for solving Eq. (2), we now proceed to discuss some physical implications of the scattering process. In the steady-state limit, $|\omega|\ll|\epsilon|$, the ratios ($\mu=0,x,y,z$)

$$T^A_{0\mu}=\mathrm{tr}(C^A_{11}\sigma^\mu)/\mathrm{tr}(C^B_{11})\,,$$
$$R^B_{0\mu}=-\mathrm{tr}(C^B_{22}\sigma^\mu)/\mathrm{tr}(C^B_{11}) \tag{4}$$

characterize the transmission and Andreev reflection of excitations incident from the B phase into the A phase. The ratios T^A_{00} and R^B_{00} have the direct interpretation as the probabilities that an incident quasiparticle will be transmitted and Andreev reflected: $T^A_{00}+R^B_{00}=1$.

It may come as a surprise to note that even an unpolarized incident beam, $\mathrm{tr}(C^B_{11}\sigma)=0$, yields a partially polarized beam of transmitted and Andreev-reflected excitations (see, however, Ref. 6). This is illustrated in

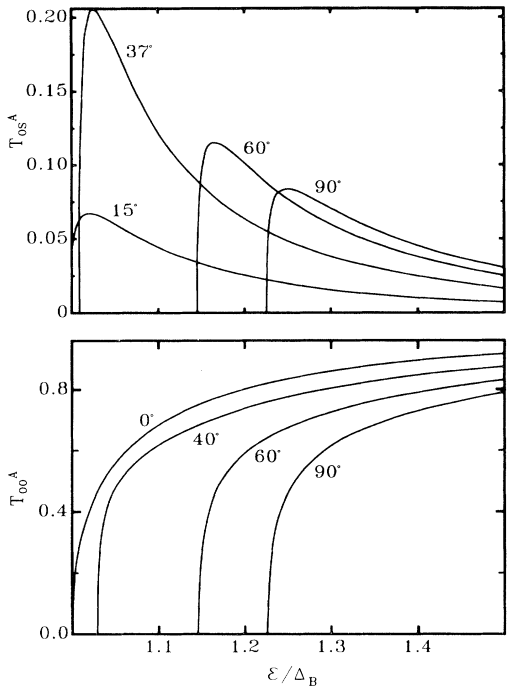

FIG. 2. Transmission of excitations from the B phase into the A phase for an unpolarized incoming beam, $\mathrm{tr}(C^B_{11}\sigma)=0$. The ratio T^A_{00} and the magnitude T^A_{0s} of the vector part, $T^A_{0\mu}=T^A_{0s}(\hat{\mathbf{k}}\times\hat{\mathbf{w}})_\mu/|\hat{\mathbf{k}}\times\hat{\mathbf{w}}|$, are plotted as functions of scaled energy $\epsilon/\Delta_B\geq1$. The orientation of the incident $\hat{\mathbf{k}}$ vector is given in nonstandard polar coordinates by $\hat{\mathbf{k}}=\cos\theta_k\hat{\mathbf{x}}+\sin\theta_k(\cos\phi_k\hat{\mathbf{y}}+\sin\phi_k\hat{\mathbf{z}})$. Curves are shown with $\theta_k=135°$, $\phi_k=0°,40°,60°,90°$ for T^A_{00} and $\theta_k=135°$, $\phi_k=15°,37°,60°,90°$ for T^A_{0s}.

Fig. 2 where we present T^A_{00} and the magnitude T^A_{0s} of the vector part of $T^A_{0\mu}$ for a range of incident $\hat{\mathbf{k}}$ vectors versus scaled energy ϵ/Δ_B. The orientation of the vector part of $T^A_{0\mu}$ is along $\hat{\mathbf{k}}\times\hat{\mathbf{w}}$, where $\hat{\mathbf{w}}$ is given in Eq. (1). Note that a necessary condition for total Andreev reflection of waves from the B phase into the A phase is $\Delta_B < |\epsilon| < \Delta_A|\hat{\mathbf{k}}\times\hat{\mathbf{l}}|$; hence $T^A_{00}=0$ in this regime as illustrated in the lower part of Fig. 2. We draw attention to the fact that even for equal bulk gaps, $\Delta_B=\Delta_A|\hat{\mathbf{k}}\times\hat{\mathbf{l}}|$ (i.e., $\hat{\mathbf{k}}\cdot\hat{\mathbf{l}}=\pm 1/\sqrt{3}$), Andreev reflection occurs.

By a change of perspective we can consider not the situation above, where a wave packet of excitations scatters off a stationary A-B interface, but rather a situation in which the interface progresses through the system. It seems natural that the moving interface will, by the mechanism described above, change the polarization of the system.

For a better understanding of recent experiments on the A-B phase boundary[3] we present next our findings on the magnetic properties of a static interface. In general such an interface is expected to be magnetically active due to the lack of time reversal of the A phase. Because the order parameter of Eq. (1) is unitary, $\Delta\times i\Delta^*=0$, no finite magnetization is found in equilibrium.[11] There exists, however, a substantial contribution to the magnetic correlations which arises from bound states and resonances of quasiparticles localized in the vicinity of the A-B phase boundary. These and other equilibrium properties of the interface are in the information carried by the retarded (advanced) quasiclassical propagators evaluated at $\omega=0$. The retarded equilibrium propagators follow from Eq. (3) with the 2×2 blocks $\tilde{C}_{mn}=\pi i\delta(\omega)C_{mn}$ as follows:

$$C_{11}=1,\quad C_{22}=-1$$

and

$$C_{21}=0,\quad C_{12}\neq 0 \text{ for } \hat{\mathbf{x}}\cdot\mathbf{R}/\hat{\mathbf{x}}\cdot\hat{\mathbf{k}}>0,$$

$$C_{21}\neq 0,\quad C_{12}=0 \text{ for } \hat{\mathbf{x}}\cdot\mathbf{R}/\hat{\mathbf{x}}\cdot\hat{\mathbf{k}}<0.$$

Assuming $\epsilon>0$, $\hat{\mathbf{k}}_x>0$, one obtains, for example,

$$g^R_{\rm eq}(x;\hat{\mathbf{k}};\epsilon)=\pi iK^B\begin{bmatrix}1 & C^B_{12}e^{2iE^Bx/v_F\hat{\mathbf{k}}_x}\\ 0 & -1\end{bmatrix}K^B \text{ for } x>0,$$
$$g^R_{\rm eq}(x;\hat{\mathbf{k}},\epsilon)=\pi iK^A\begin{bmatrix}1 & 0\\ C^A_{21}e^{-2iE^Ax/v_F\hat{\mathbf{k}}_x} & -1\end{bmatrix}K^A \text{ for } x<0. \tag{5}$$

In the interval $|\epsilon|<\min(\Delta_B,\Delta_A|\hat{\mathbf{k}}\times\hat{\mathbf{l}}|)$ the parts of $g^R_{\rm eq}$ proportional to $C^B_{12}C^A_{21}$ decay exponentially with distance, leaving for $|x|\to\infty$ the bulk propagator $\pi i\mathcal{H}/E$. The continuity of $g^R_{\rm eq}$ at $x=0$ fixes the unknowns C^B_{12},C^A_{21} *uniquely* in terms of the 2×2 blocks of the overlap K^AK^B.[9] The exponentially decaying parts of the retarded propagator correspond to bound states of quasiparticles confined to the A-B phase boundary.[12] The bound states have energies $\epsilon_b^{\pm}$ given by poles of C^B_{12} and C^A_{21} on the real ϵ axis. They exist when the $\hat{\mathbf{k}}$ vector satisfies the inequalities

$$\min(\Delta_B^2,\Delta_A^2|\hat{\mathbf{k}}\times\hat{\mathbf{l}}|^2)>(\epsilon_b^{\pm})^2>\Delta_B[a_1\hat{\mathbf{k}}\cdot\hat{\mathbf{w}}\mp a_2|\hat{\mathbf{k}}\times\hat{\mathbf{w}}|]$$

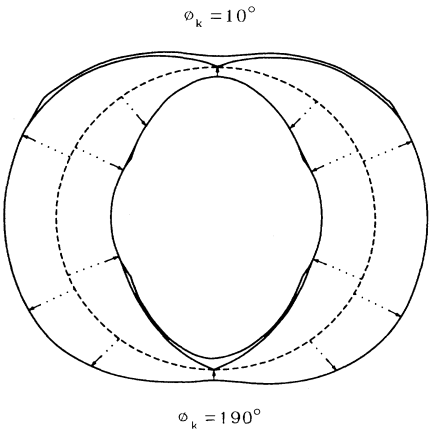

FIG. 3. Energies of bound states localized in the vicinity of the A-B phase boundary for a wide range of $\hat{\mathbf{k}}$ orientations. The innermost and outermost lines indicate schematically $\epsilon_F\pm\Delta(\hat{\mathbf{k}})$ where $\Delta(\hat{\mathbf{k}})$ is the minimum of the bulk gaps. All bound-state energies $\epsilon_b^{\pm}$ lie within these lines and are given by the solid curves. Arrows indicate where the branches of the bound state terminate. Curves are shown for $\phi_k=10°$ (upper hemisphere) and $\phi_k=190°$ (lower hemisphere) vs polar angle θ_k. The orientation of $\hat{\mathbf{k}}$ is given in nonstandard coordinates by $\hat{\mathbf{k}}=\cos\theta_k\hat{\mathbf{x}}+\sin\theta_k(\cos\phi_k\hat{\mathbf{y}}+\sin\phi_k\hat{\mathbf{z}})$.

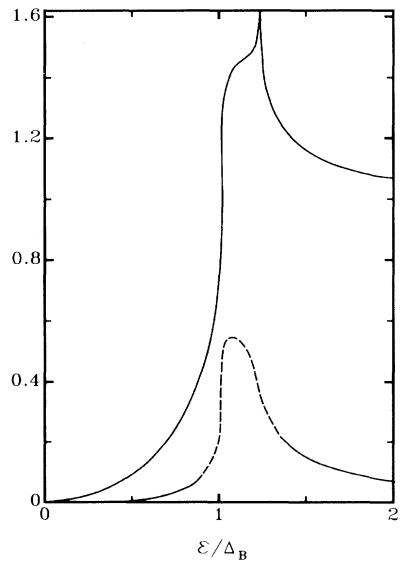

FIG. 4. Solid-angle-$\hat{\mathbf{k}}$-integrated density spectral function $n(x,\epsilon)$ (full line) and spin spectral function $-m_y(x,\epsilon)$ (dashed line) vs scaled energy ϵ/Δ_B for $x=0$.

and take the following analytic form:

$$\epsilon_b^{\pm} = \Delta_B(a_2\hat{\mathbf{k}}\cdot\hat{\mathbf{w}} \pm a_1|\hat{\mathbf{k}}\times\hat{\mathbf{w}}|)/[(a_1-\Delta_B\hat{\mathbf{k}}\cdot\hat{\mathbf{w}})^2+(a_2\pm\Delta_B|\hat{\mathbf{k}}\times\hat{\mathbf{w}}|)^2]^{1/2}, \quad (6)$$

where $a_1+ia_2=\Delta_A\hat{\mathbf{k}}\cdot(\hat{\boldsymbol{\phi}}_1+i\hat{\boldsymbol{\phi}}_{II})$, as defined in Eq. (1).

As is clearly demonstrated in Fig. 3 the bound-state energies are quite close to the effective gap, $\min(\Delta_B, \Delta_A|\hat{\mathbf{k}}\times\hat{\boldsymbol{l}}|)$, for a wide range of $\hat{\mathbf{k}}$ orientations. Under these circumstances (see, however, Ref. 13) the exact profile of the order parameter near $x\simeq 0$ becomes irrelevant and the bound states extending over many coherence lengths are correctly described by $\epsilon_b^{\pm}$ as stated above.

It should be noted that the bound states, labeled by $\hat{\mathbf{k}}$, are excluded from a cone of $\hat{\mathbf{k}}$ vectors corresponding to $\arccos(\hat{\mathbf{k}}\cdot\hat{\mathbf{x}})\lesssim 17°$.

The upper diagonal 2×2 block of $g_{eq}^{R(A)}$ determines the spectral functions for the density and the spin:

$$n=\mathrm{tr}[(g_{eq}^A-g_{eq}^R)_{11}]/2\pi i$$

and

$$m_a=\mathrm{tr}[(g_{eq}^A-g_{eq}^R)_{11}\sigma^a]/2\pi i\,.$$

Any "golden-rule"-related calculation may be expressed in terms of convolutions of these spectral functions and as such they provide important ingredients for the understanding of the A-B phase boundary. Note that the advanced propagator appearing above, g_{eq}^A, does not contain new information and may be found from the following general symmetries:[8]

$$g^A(\mathbf{R},t;\hat{\mathbf{k}},\epsilon)=[\tau_3 g^R(\mathbf{R},t;\hat{\mathbf{k}},\epsilon)\tau_3]^{\dagger},$$

$$g^R(\mathbf{R},t;-\hat{\mathbf{k}},-\epsilon)=[\tau_2 g^A(\mathbf{R},t;\hat{\mathbf{k}},\epsilon)\tau_2]^{\mathrm{tr}}.$$

In Fig. 4 we show the results for the solid-angle-$\hat{\mathbf{k}}$-integrated spectral functions $n(x,\epsilon)=\int(d\Omega/4\pi)n(x;\hat{\mathbf{k}},\epsilon)$ and $\mathbf{m}(x,\epsilon)=\int(d\Omega/4\pi)\mathbf{m}(x;\hat{\mathbf{k}},\epsilon)$ evaluated at the interface $x=0$; we find that $m(0,\epsilon)$ is oriented along $\hat{\boldsymbol{l}}=-\hat{\mathbf{y}}$.

Note that we have presented these quantities for $\epsilon>0$ only, since they are even in ϵ. Besides the density and the spin spectral functions we have also calculated the mass current j_a and the spin current $j_{\mu a}$. We predict that both of these observables have finite components $j_z\neq 0$ and $j_{yx}\neq 0$, $j_{yz}\neq 0$, and $j_{zy}\neq 0$. The origins of these nonvanishing currents are the bound states and resonances generated by the matching of a rank-1 tensor (A phase) to a rank-3 tensor (B phase).

To summarize, in this paper we have presented an outline of the ways the A-B phase boundary can influence both ballistic excitations and equilibrium properties. The calculational details and further results will be published elsewhere.

It is a pleasure to thank G. Barton, G. Eilenberger, M. Krusius, J. Kurkijärvi, A. J. Leggett, P. Nozières, M. Salomaa, P. Thalmeier, E. Thuneberg, and W. Zhang for helpful discussions. This research was supported in part by the Science and Engineering Research Council, United Kingdom.

[a]Permanent address: Physics Division, School of Mathematical and Physical Sciences, University of Sussex, Brighton BN1 9QH, Sussex, United Kingdom.

[1]For example, D. M. Lee and R. C. Richardson, in *The Physics of Liquid and Solid Helium, Part II* edited by K. H. Bennemann and J. B. Ketterson (Wiley, New York, 1978).

[2]D. D. Osheroff and M. C. Cross, Phys. Rev. Lett. **38**, 905 (1977).

[3]D. S. Buchanan, G. W. Swift, and J. C. Wheatley, Phys. Rev. Lett. **57**, 341 (1986).

[4]N. Schopohl, Phys. Rev. Lett. **58**, 1664 (1987).

[5]S. Yip, Phys. Rev. B **35**, 8733 (1987).

[6]G. Kieselmann and D. Rainer, Z. Phys. B **52**, 267 (1983).

[7]S. Yip, Phys. Rev. B **32**, 2915 (1985); Ph.D. thesis, University of Illinois at Urbana-Champaign, 1986 (unpublished).

[8]J. Serene and D. Rainer, Phys. Rep. **101**, 221 (1983).

[9]N. Schopohl and D. Waxmann, in Proceedings of the Conference on Quantum Fluids and Solids, Gainesville, Florida, 24–28 April 1989 (American Institute of Physics, New York, to be published); to be published.

[10]A. F. Andreev, Zh. Eksp. Teor. Fiz. **46**, 1823 (1964) [Sov. Phys. JETP **19**, 1228 (1964)].

[11]A small magnetization results if the exact order parameter of Ref. 4 is used.

[12]Bound states at the A-B interface are briefly mentioned by Yip in his thesis (Ref. 7).

[13]For $|\hat{\mathbf{k}}\cdot\hat{\mathbf{x}}|\ll 1$ the energy $|\epsilon_b^{\pm}|$ is small, such that the localization range of the bound states is comparable to or shorter than the thickness of the phase boundary. Then a more elaborate description using the exact profile of the order parameter is necessary. For these states a spin splitting of the bound-state energies is expected due to $\Delta\times i\Delta^*\neq 0$ as found in Ref. 4.